A Simulation and Experiment Concerning the Solidification of an Al-Zn Alloy Casting

BEDO Tibor
Transilvania University of Brasov, Romania, bedo.tibor@unitbv.ro
DĂIAN Marcel
Transilvania University of Brasov, Romania, marceldaian@yahoo.com
VARGA Bela
Transilvania University of Brasov, Romania, varga.b@unitbv.ro
STOICĂNESCU Maria
Transilvania University of Brasov, Romania, stoican.m@unitbv.ro
CRIŞAN Aurel
Transilvania University of Brasov, Romania, crisan.a@unitbv.ro
CIOBANU Ioan
Transilvania University of Brasov, Romania, ciobanu_i_bv@yahoo.com

Abstract
A software product was developed to simulate the solidification of rotationally symmetrical castings. It applies to gravity and centrifugally cast alloys that solidify within a temperature interval. The software uses a mathematical model with finite differences and cylindrical coordinates. An experimental verification of this software is presented. The simulated cooling curves obtained by this software are compared to those obtained experimentally by thermal analysis. The verification was carried out for the case of a cylindrical hollow part cast from an aluminium-zinc alloy. The experimental results are very close to those obtained by simulation. This confirms the validity of software.

Keywords
solidification simulation, casting, thermal analysis, aluminium-zinc alloy

1. Aim

To date several simulation software products for the solidification of castings have been developed at Transilvania University of Braşov. Recently a simulation software product has been devised for the solidification of rotationally symmetrical parts cast from alloys of solid solution solidification type. The software is developed in cylindrical coordinates and is applicable to gravity or centrifugally cast parts. For this type of parts the utilization of cylindrical coordinates allows a significant decrease of simulation time. Experimental thermal analysis was deployed in order to verify the accuracy of the results provided by this software for several cast alloys. For this purpose, the experimentally obtained variation curves of temperature in various points of a mould – cast part system were recorded. These were compared to similar simulated curves, obtained by means of the software undergoing verification. The paper presents the results of the software verification for a part gravity cast from an Al-Zn alloy.

2. Working Method

The part was cast from Al - 10%Zn, a binary alloy with solid solution solidification within a temperature interval. Figure 1 shows the dimensions of the mould – cast part assembly considered for verification. The cylindrical tube shaped part has a wall thickness of b=30mm and an exterior diameter of D = 120 mm. According to the Al - Zn thermal equilibrium diagram shown in figure 2, the liquidus temperature of this alloy is of 640 °C, and the solidus temperature of 620 °C. Table 1 features the chemical composition of the alloy used for experiments. Three thermocouples were mounted in the casting mould: one at 2 mm distance from the exterior surface of the part, another one on the axis of the part wall (at 15mm distance from the exterior surface of the part) and the third one in the wall of the mould, at 2mm distance from the exterior surface of the part. The thermocouples were placed at half height of the cast part. Figure 1 displays the location of the thermocouples in the mould.

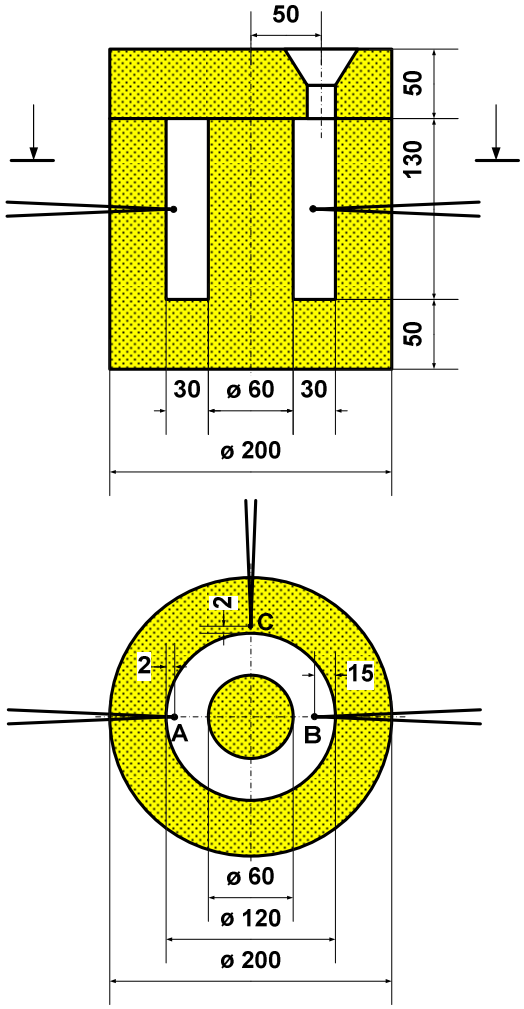

Fig. 1. Casting - mould assembly

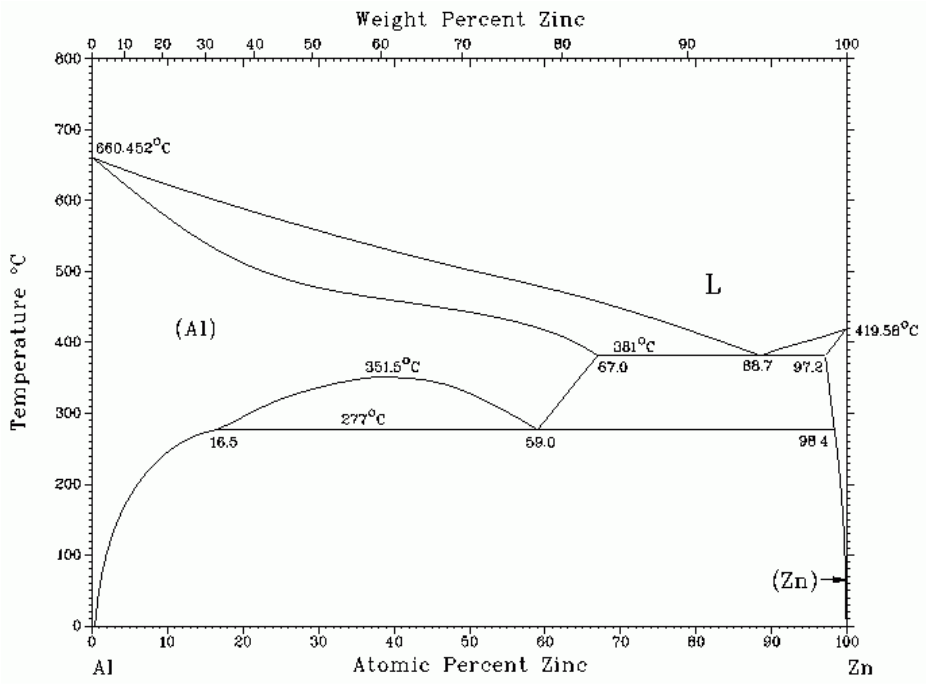

Fig. 2. Al - Zn binary diagram of thermal equilibrium

Table 1. Chemical composition of the experimentally cast AlZn10 alloy

No.	Element	Element content			
		Measurement1	Measurement 2	Measurement 3	Mean
	Symbol	%	%	%	%
1	Al	91.467	91.379	91.486	91.444
2	Zn	8.115	8.226	8.144	8.162
3	Si	0	0	0	0
4	Cu	0.183	0.183	0.183	0.183
5	Mn	0	0	0	0
6	Mg	0	0	0	0
7	Cr	0	0.001	0	0.0003
8	Fe	0.092	0.060	0.040	0.064
9	Ti	0.058	0.061	0.060	0.060
10	Pb	0	0	0	0
11	Sn	0.027	0.030	0.027	0.028
12	Ni	0	0	0	0
13	V	0.058	0.061	0.060	0.060

3. Experimental Results

Figures 3 show images from the casting process and the set-up for data recording onto the thermal analysis device. Figure 4 shows the temperature variation curves determined experimentally by means of the thermocouples. Figure 5 shows the graphs of the cooling curve derivatives for points A and B of the part. The temperature of the cast alloy at the initial moment of the thermal analysis (the initial moment of the cast liquid alloy cooling in the mould) was determined based on the numerical results recorded by means of the thermocouples. Further determined were the temperature and the beginning and end of solidification times in the two considered points of the part. Table 2 shows these values.

Table 2. Experimental results in points A and B of the casting

No.	Point of measuring	Initial temperature	Beginning of cooling time	Beginning of solidification temperature	Solidus temperature	Beginning of solidification time	End of solidification time	Cooling time in liquid state	Solidification time
	Symbol	T_0	t_0	T_L	T_{Eexp}	t_{0L}	t_{SS}	$\Delta t_L = t_{0L}-t_0$	$\Delta t_S = t_{SS}-t_{0L}$
	u.m.	°C	s	°C	°C	s	s	s	s
1	point "A" at 2mm distance from the exterior surface	644.037	170	618.031	618.031	249	1459	79	1200
2	point "B"at 15mm distance from the exterior surface	707.922	169	640.609	619.536	423	1514	254	1260

The experimental curves highlight the beginning of solidification temperature. The end of solidification temperature is more difficult to reveal on the temperature variation curves for alloys of solid solution solidification type, because of the constitutional undercooling occurring at the end of solidification. The end of solidification temperature is easier highlighted on the temperature time derivative curves. In this case the experimental curves and the numerical results highlighted for the

alloy cast into test pieces the beginning of solidification temperature (liquidus) T_{Lexp}=640 °C and the end of solidification temperature (solidus) T_{Sexp}=620 °C. These correspond to a solidification interval of ΔTs=20 °C.

a. mould making

b. mould cavity

c. position of "B" thermocouple

d. temperature measuring and recording installation

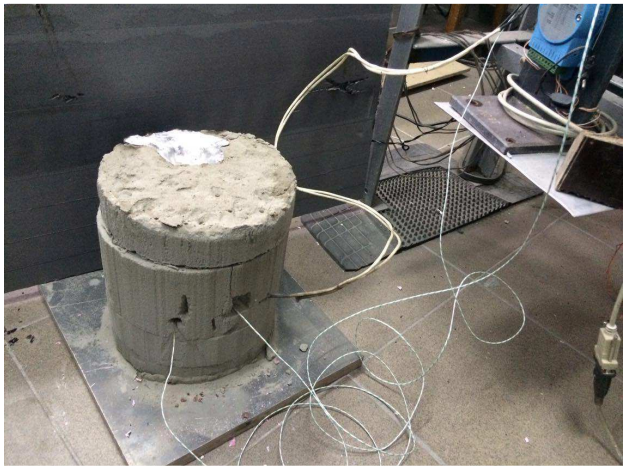

e. solidification of the cast alloy

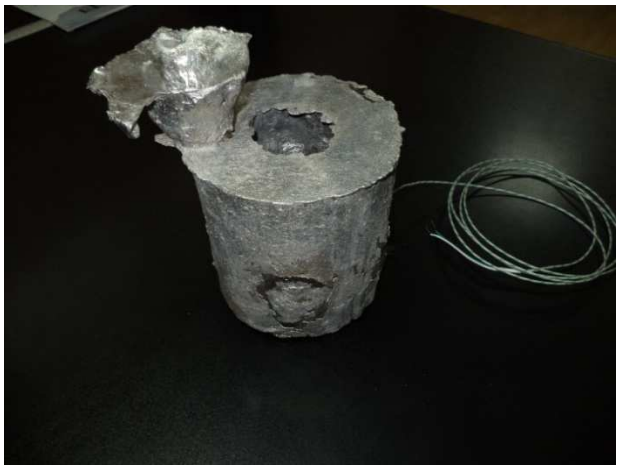

f. set casting

Fig. 3. Casting of the experimental test piece

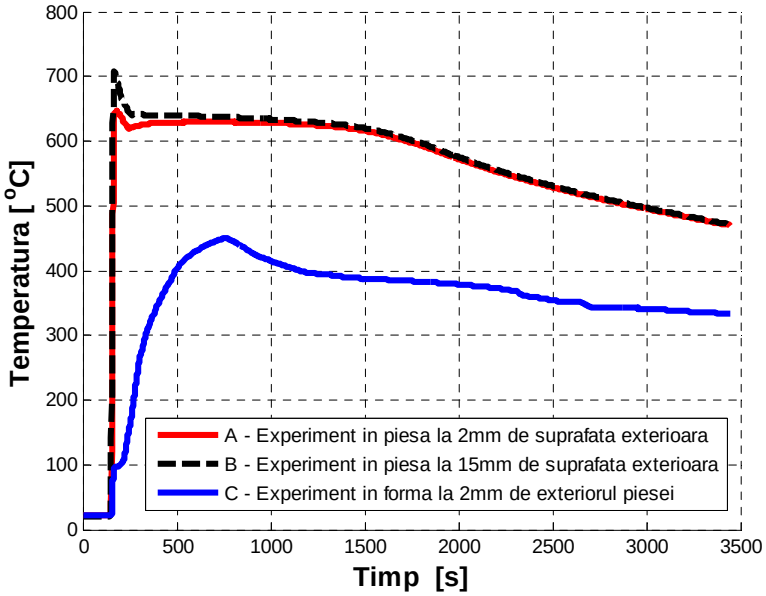

Fig. 4. Experimentally recorded temperature variation (AlZn10 alloy)
A – point in the part at 2mm distance from the exterior surface of the part;
B – point in the part at 15 mm distance from the exterior surface;
C – point in the mould at 2mm distance from the exterior surface of the part

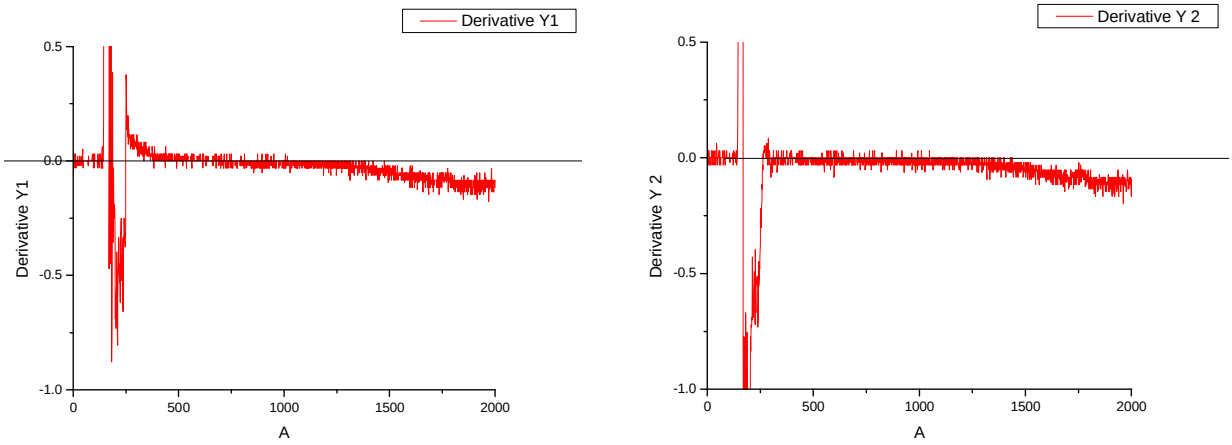

a) point A in the cast part, at 2 mm distance from the exterior surface of the part

b) point B in the cast part, at 15mm distance from the exterior surface of the part

Fig. 5. Temperature time derivative (experimental results)

4. Comparison of Simulated and Experimental Results

In order to verify the developed software product the results obtained by experimental thermal analysis were compared to those obtained by simulation of solidification. For this purpose the cooling and solidification of the part that was actually cast experimentally were simulated (tube shaped cylindrical part of interior diameter d_{int}=60mm and wall thickness B=30mm, as shown in figures1 and 3f). The values indicated in table 3 were considered for the thermo-physical characteristics of the Al-Zn alloy. For the simulation, the liquidus temperature experimentally measured in point A was used, which is close to the one determined on the equilibrium curve. The solidus temperature used in simulation was the one provided by the diagram of equilibrium, as the software does not simulate constitutional undercooling and does not reveal the real solidus temperature. Figure 6 shows the temperature variation curves obtained by simulation for the three points (A, B, and C). For a better comparison of the simulated and experimental results, figures 7 to 9 show on the same graph, the curves obtained by both simulation and experimentally.

Table 3. Geometrical and thermo-physical characteristics used in simulation

No.	Parameter	Symbol	Unit of measure	Value
1	Exterior diameter of part	D	m	0.12
2	Interior diameter of part	d	m	0.06
3	Part length	L	m	0.13
4	Exterior diameter of mould	L_{Fo}	m	0.20
5	Pitch of mould mesh	Δ	m	0.001
6	Time increment	τ	s	0.005
7	Environment temperature	Tex	°C	20
8	Coefficient of heat exchange with the environment	αex	$W/m^2/K$	12
9	Liquidus temperature of the alloy	Tsme	°C	640
10	Solidus temperature of the alloy	Tsme	°C	620
11	Coefficient of thermal conductivity of the mould	λsfo	W/m/K	0.6
12	Coefficient of thermal conductivity of the solid alloy	λsme	W/m/K	200
13	Coefficient of thermal conductivity of the liquid alloy	λlme	W/m/K	100
14	Specific heat of the mould	Csfo	J/kg/K	1000
15	Specific heat of the liquid alloy	Clme	J/kg/K	1200
16	Specific heat of the solid alloy	Csme	J/kg/K	1000
17	Mould density	ρfo	Kg/m^3	1550
18	Liquid alloy density	ρme	Kg/m^3	2600
19	Latent solidification heat of the alloy	Lme	J/kg	530000
20	Initial temperature of the mould	T0fo	°C	20
21	Initial temperature of the liquid alloy	T0me	°C	708

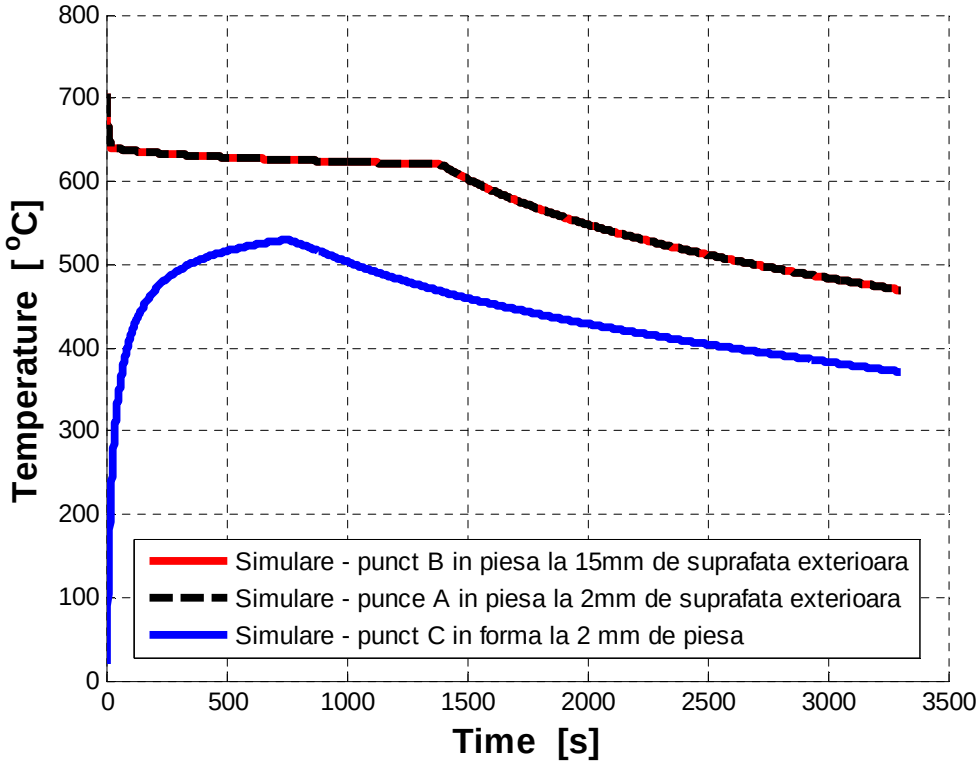

Fig. 6. Simulated temperature variation for the casting from AlZn10 alloy
A – point in the part at 2mm distance from the exterior surface of the part;
B – point in the part at 15 mm distance from the exterior surface;
C – point in the mould at 2mm distance from the exterior surface of the part

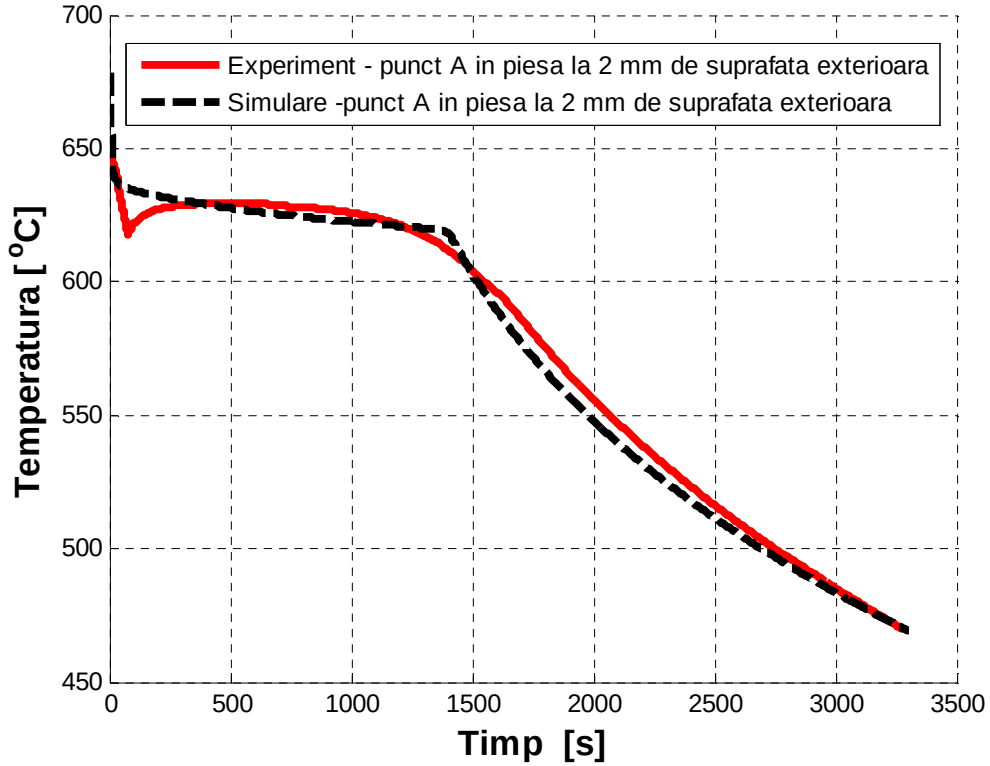

Fig. 7. Experimental and simulated temperature variation for point "A" located in the cast part, at 2 mm distance from the exterior surface of the part
(— experiment, --- simulation)

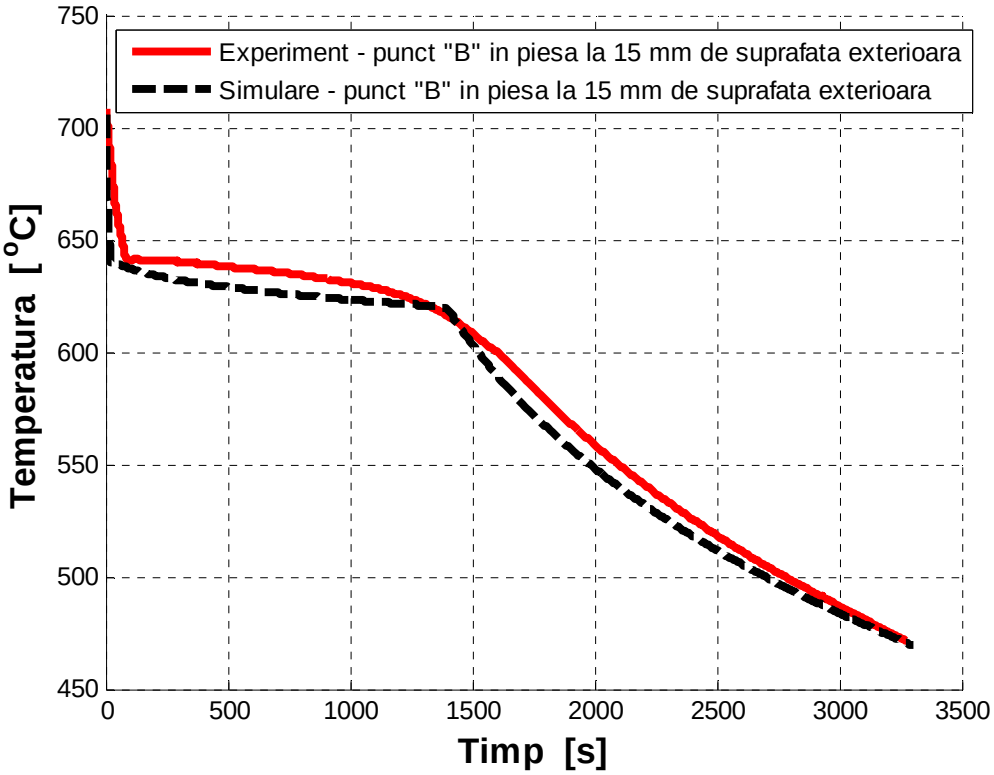

Fig. 8. Experimental and simulated temperature variation for point "B" located in the cast part, at 15 mm distance from the exterior surface of the part
(— experiment, --- simulation)

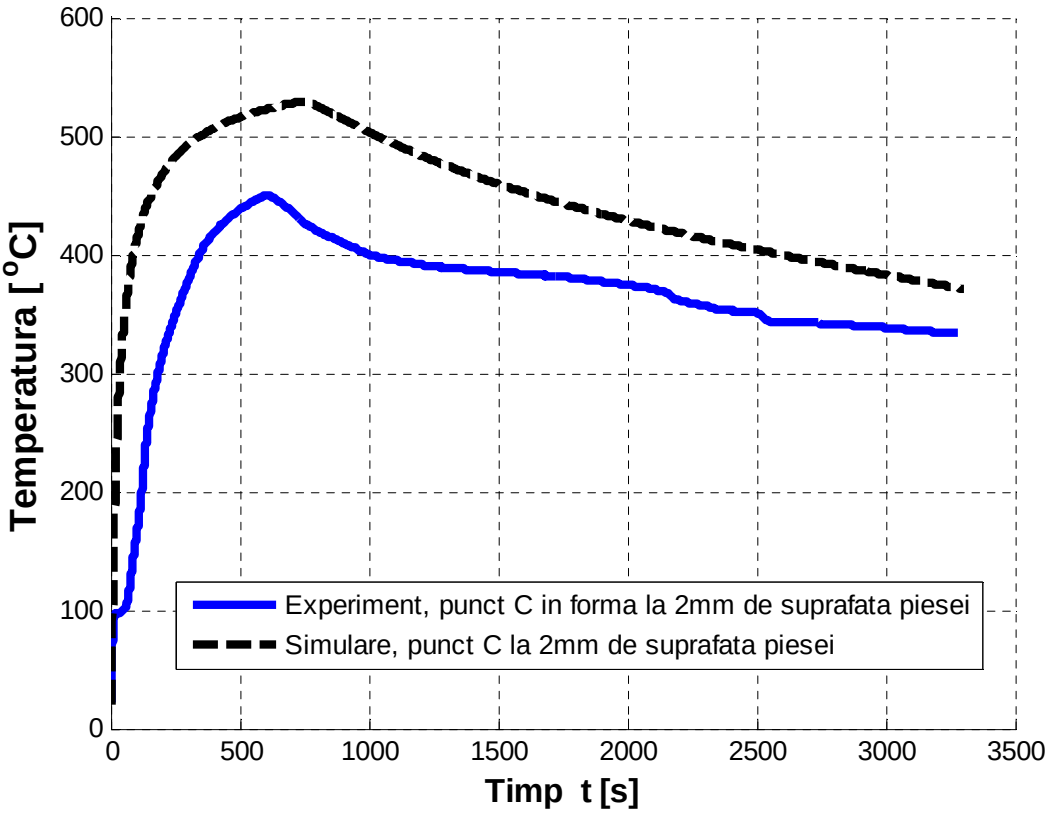

Fig. 9. Experimental and simulated temperature variation for point "C" located in the mould, at 2 mm distance from the exterior surface of the part
(— experiment, --- simulation)

Figures 7 to 9 show a good agreement between the simulated results and those obtained by experimental thermal analysis in both points ("A" and "B") located in the casting. Small differences occur in the area of liquidus cooling of the alloy and in the area of end of solidification. The differences in the liquidus area can be explained by possible deviations of the values of certain thermo-physical parameters (specific heat, thermal conductivity of the alloy in liquidus state) used in simulation. In the case of point A, a small difference in the area of beginning of solidification can be noticed. This is explained by the stronger undercooling of the alloy in this point, which is located in the immediate vicinity of the mould. Because of a higher cooling rate in the first moments of contact with the mould, the undercooling at the beginning of solidification is greater. The software does not simulate this undercooling, what explains the difference between the experimental and simulated curves in this area in point A. The small differences in the end of solidification area are explained by the constitutional undercooling of the alloy that occurs towards the end of the real solidification. This undercooling is also not reflected by the simulation software.

In the case of point C (figure 9) located in the mould wall at 2mm distance from the exterior surface of the casting a significant difference occurs between the simulated and experimental curves. The curves have similar shapes and peak at the same time value. The values of the experimentally measured temperatures are about 10-15% smaller than the simulated ones. This difference can be explained on one hand by the imperfect contact between the thermocouple and the mould wall. The imperfect contact is caused by the thermocouple not having been attached in the mould wall during mould making. The thermocouple was introduced into a hole drilled into the mould wall subsequently to the making of the mould. Another explanation of the experiment – simulation difference (in this point „C") is the repair of the mould wall consisting of a thin layer of a sand and wet clay mixture in the area of the tip of this thermocouple (the area of point „C"). The evaporation of the humidity from this layer has absorbed a latent heat of vaporization (also noticeable on the experimental curve in point C – in figures 4 and 9).

5. Conclusions

The experimental results obtained by thermal analysis demonstrate that SIM-SOLSOL CIL software provides realistic data concerning the solidification of castings (solidification time and temperature distribution on the part wall) from alloys with solid solution type solidification within a temperature interval. Consequently the software product developed at Transilvania University based on cylindrical coordinates can be used with sufficient precision in theoretical and concrete applied research, as well as in the design of casting technologies of rotationally symmetrical parts, including centrifugally cast ones.

References

1. Ciobanu, I., Munteanu, S.I., Crişan, A. (2004): *Model mathematic şi soft 3D bazat pe metoda diferenţelor finite pentru simularea solidificării pieselor turnate din aliaje eutectice* (*Mathematical Model and 3D Software on Finite Differences Based for the Simulation of Castings from Eutectoid Alloys*). Metalurgia, ISSN 0461-9579, vol. 56, no. 12, p. 17-24 (in Romanian)
2. Ciobanu, I., Monescu, V., Munteanu, S.I., Crişan, A. (2010): *Simularea 3D a solidificării pieselor turnate* (*3D Simulation of Castings Solidification*). Editura Universităţii Transilvania din Braşov, ISBN 978-973-598-678-0, Brasov, Romania (in Romanian)
3. Ionescu, I., Dăian, M., Ciobanu, I., Varga, B., Bedo, T., Stoicănescu, Maria (2016): *Experimental Verification of a Software for Simulation of Centrifugal Casting Solidification*. **RECENT**, ISSN 1582-0246, vol. 17, no. 1(47), p. 26-32
4. Ionescu, I., Ionescu, Daniela, Ciobanu, I., Jiman, V. (2012): *Computation of the Heat Exchange Coefficient in Cylindrical Coordinates Mathematical Modeling of Castings Solidification*. **RECENT**, ISSN 1582-0246, vol. 13, no. 3(36), p. 307-316
5. Soporan, V., Constantinescu, V. (1995): *Modelarea la nivel macrostructural a solidificării aliajelor* (*Macrostructural Modelling of Alloy Solidification*). Editura Dacia, ISBN 973-35-0526-9, Cluj-Napoca, Romania (in Romanian)
6. Soporan, V., Constantinescu, V., Crişan, M. (1995): *Solidificarea aliajelor (Alloy Solidification)*. Transilvania Press, ISBN 973-9704-1-5, Cluj-Napoca, Romania (in Romanian)
7. Ştefănescu, D. (2009): *Science and Engineering of Casting Solidification*. Department of Material Engineering, University of Alabama, Tuscalosa (USA), Springer US, ISBN 0-306-46750-X, ISBN 978-0-387-74609-8
8. Changrapa, K.G. (1989): *Propriétés des phases thermiques des sables auto-durcissant liés au silicate de soude*. Fonderie, Fondeurd'aujourd'hui, ISSN 0249-3136, no. 83, p. 25-34 (in French)
9. Pehlke, R.D., Jeyarajan, A., Wada, H. (1982): *Summary of thermal properties of castings alloys and mould materials*. NSF and Applied Research Division USA, p. 143-160

Received in June2016